Supplement to:

The Spatial Structure of a Nonlinear Receptive Field

Gregory W. Schwartz, Haruhisa Okawa, Felice A. Dunn, Josh L. Morgan, Daniel Kerschensteiner, Rachel O. Wong, and Fred Rieke

Nature Neuroscience: doi:10.1038/nn.3225

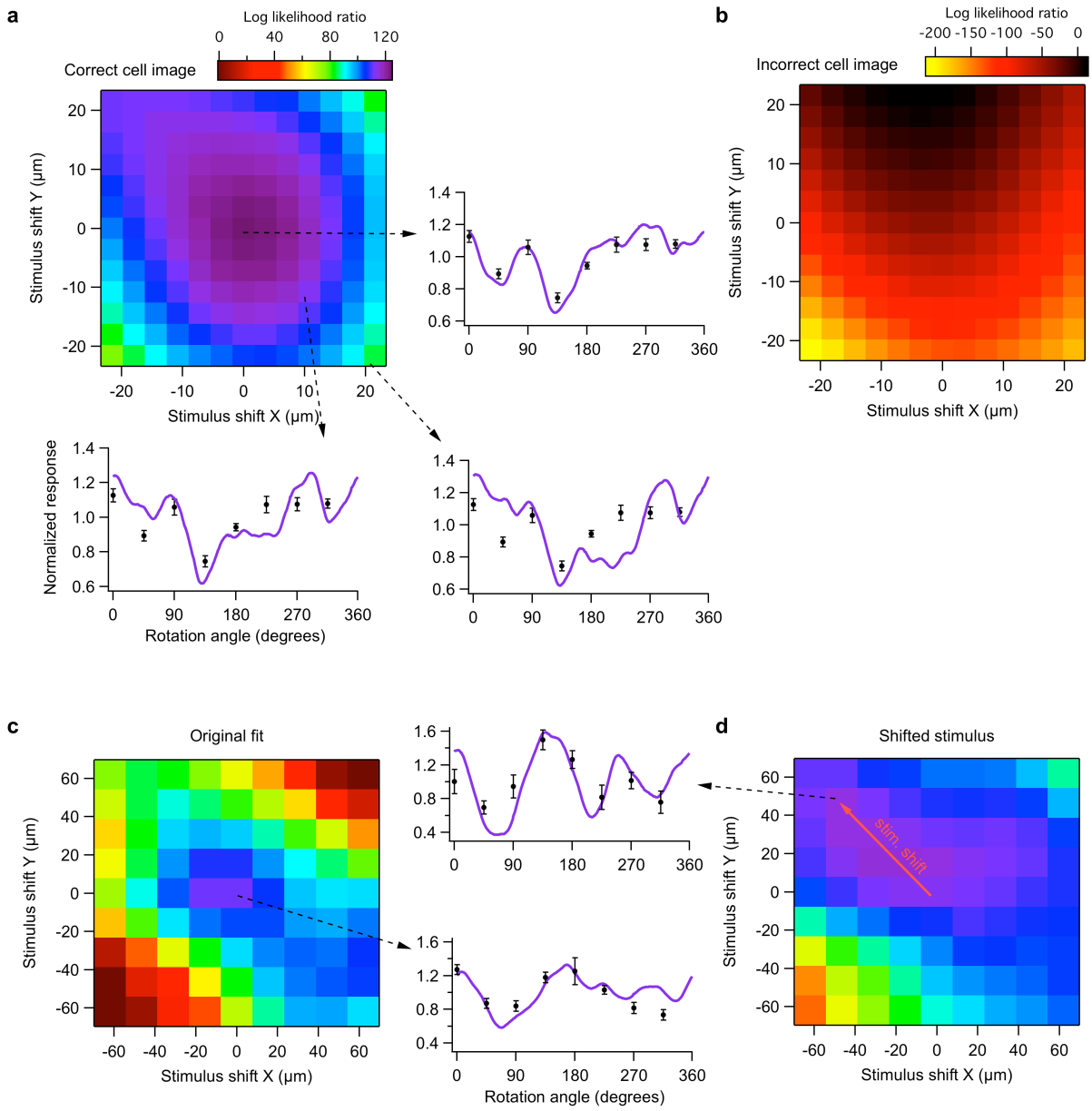

Figure S1. Accounting for a translational shift between photoreceptors and RGC dendrites. **a**, Log likelihood ratio (base 10) of the predictions of the anatomical-weights vs. the null prediction (see Methods) for small shifts in the modeled stimulus position with respect to the image of the RGC dendrites. Arrows point to example fits at 3 different modeled stimulus positions. **b**, Log likelihood ratios calculated for a model with substituted bipolar cell weights derived from a different RGC image. Note the different color scale. Data in **a** and **b** are from the cell labeled cell #1 in figure 6d. **c**, Log likelihood ratio plot as in **a** for a different cell over a larger range of model stimulus shifts. Model prediction at the best fitting stimulus position is shown. **d**, Model fits to data from the same cell as in **c**, with the actual texture stimulus shifted -48 µm in X and +48 µm in Y. Model prediction shown was not independently fit; it represents the X and Y shifts used in the experiment. Color scale is the same in **a**, **c**, and **d**. Error bars are standard deviation.

Nature Neuroscience: doi:10.1038/nn.3225

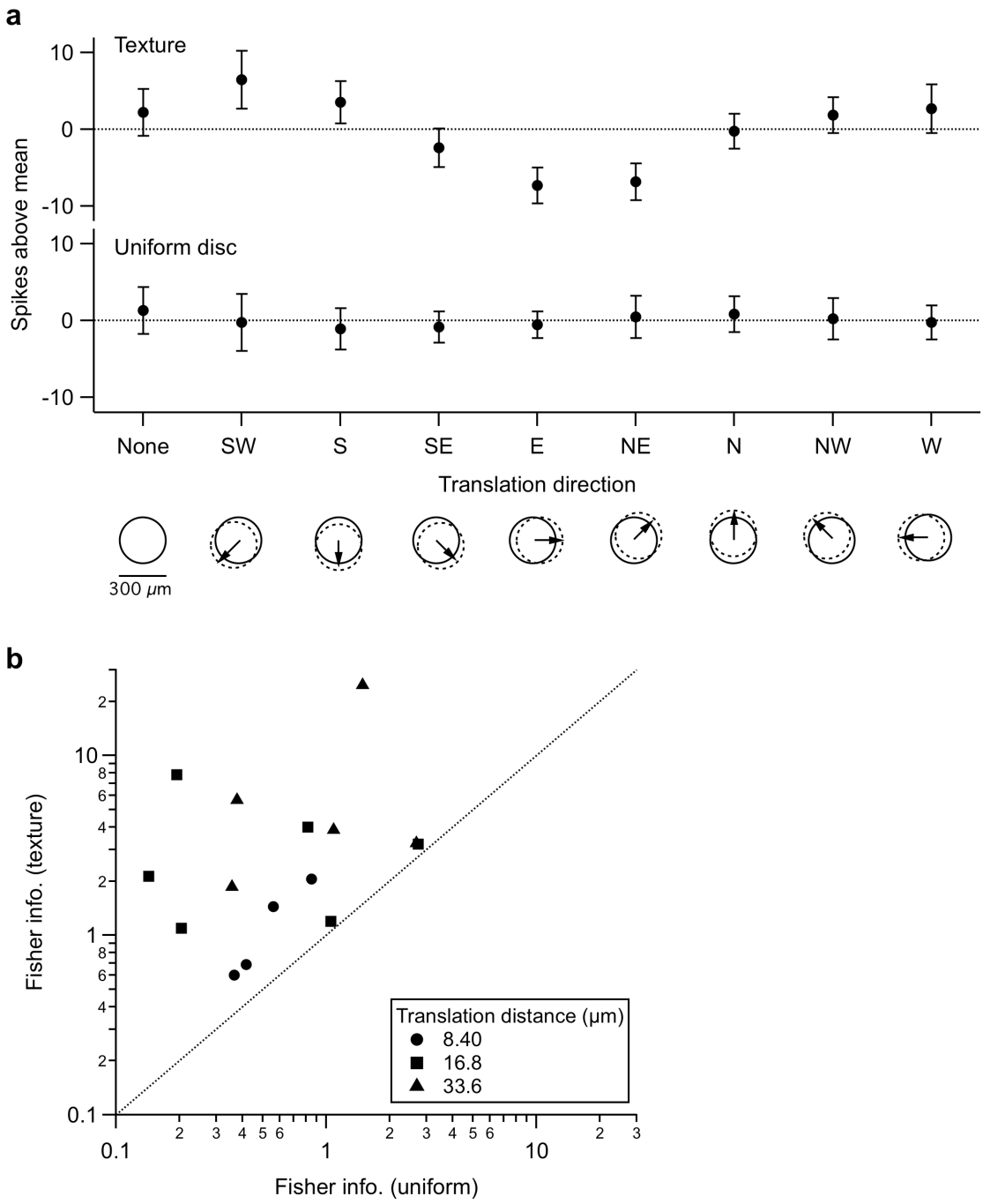

Figure S2. Sensitivity to small translations of a texture stimulus. **a**, Responses of an example cell to 33.6 μm translations of a texture pattern. Spike count above the mean in response a texture pattern (*top*) and for a uniform disc of the same size (*bottom*) at each stimulus location. The contrast of the uniform disc was adjusted to approximately match the mean spike count in response to the texture pattern. For this example uniform disc was 36% contrast, the mean spike count for the textures was 15 spikes, and the mean spike count for the uniform disc was 30 spikes. Texture scale was 36 μm. Error bars are standard deviation. **b**, Linear Fisher information in the spike count about translation direction (see Methods) for uniform discs and textures. Symbols represent different translation distances. Mean spike counts in response to texture patterns and uniform discs were 23 ± 7 and 27 ± 10, respectively.

Nature Neuroscience: doi:10.1038/nn.3225

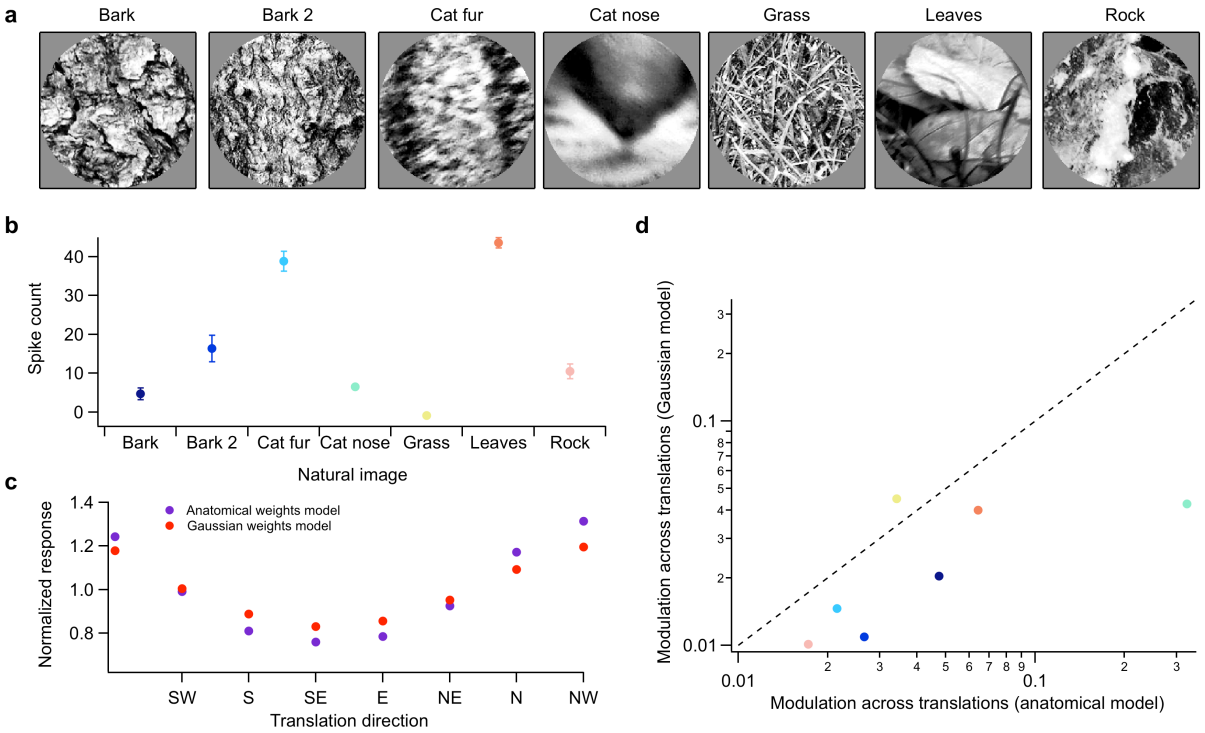

Figure S3. Fine-scale heterogeneities in bipolar weights lead to enhanced sensitivity to small translations of natural images. **a**, The natural texture stimuli that were presented to the retina and the model. As with artificial texture stimuli, the light levels were renormalized to a uniform distribution from 0 to 100% contrast with mean equal to the background. **b**, Spike counts from an On alpha-like RGC in response to each of the natural textures. Error bars are s.e.m. The response modulation likely reflects a combination of the different spatial scales present in the images (as demonstrated in Fig. 2a,b) and fine-scale heterogeneities in the RGC receptive field (Fig. 2 c-e) **c**, Model responses to 15 μm translations of the "bark" image for both the anatomical weights model (purple) and the Gaussian weights model (red). **d**, Modulation of the model, measured as the variance of the normalized model response across the eight translation directions, for each of the natural textures. Colors are as in **b**. Dashed line is unity.

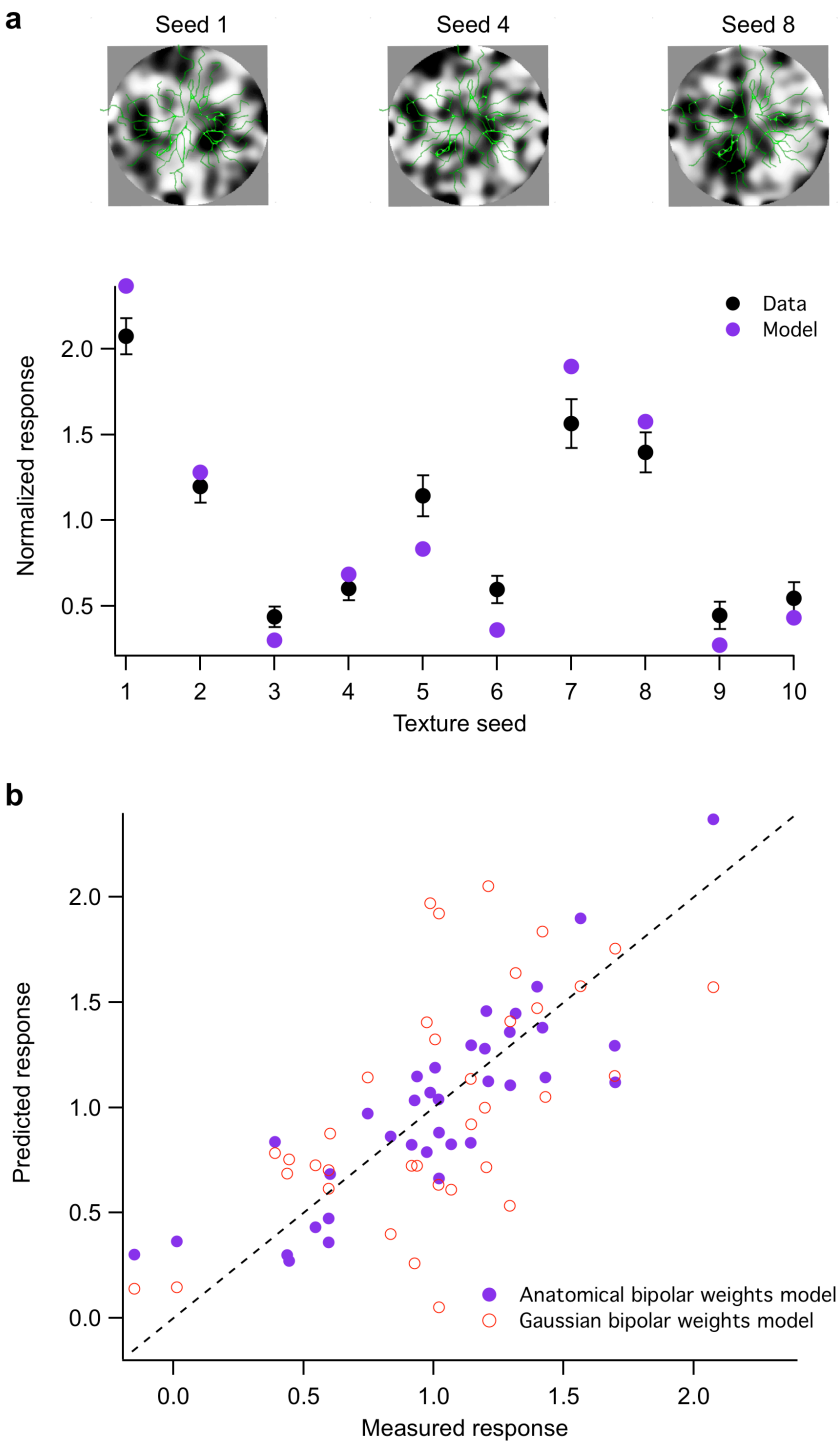

Figure S4. Sensitivity to arbitrary texture patterns. **a**, *top*, Traced RGC dendrites aligned, scaled, and superimposed on 3 of the stimuli used in the experiment. Texture scale was 25 μm. *bottom*, Normalized charge transfer in excitatory input currents (black points) for the cell pictured above in response to 10 different random textures along with model predictions (purple). Error bars are standard deviations. **b**, Measured responses and model predictions from the anatomical-weights (purple) and the Gaussian bipolar weights model (red; see Fig. 8). Dashed line is unity. Predictions from the anatomical-weights were 10^{151} more likely than those of the Gaussian model (n = 4 cells; 28 total textures).

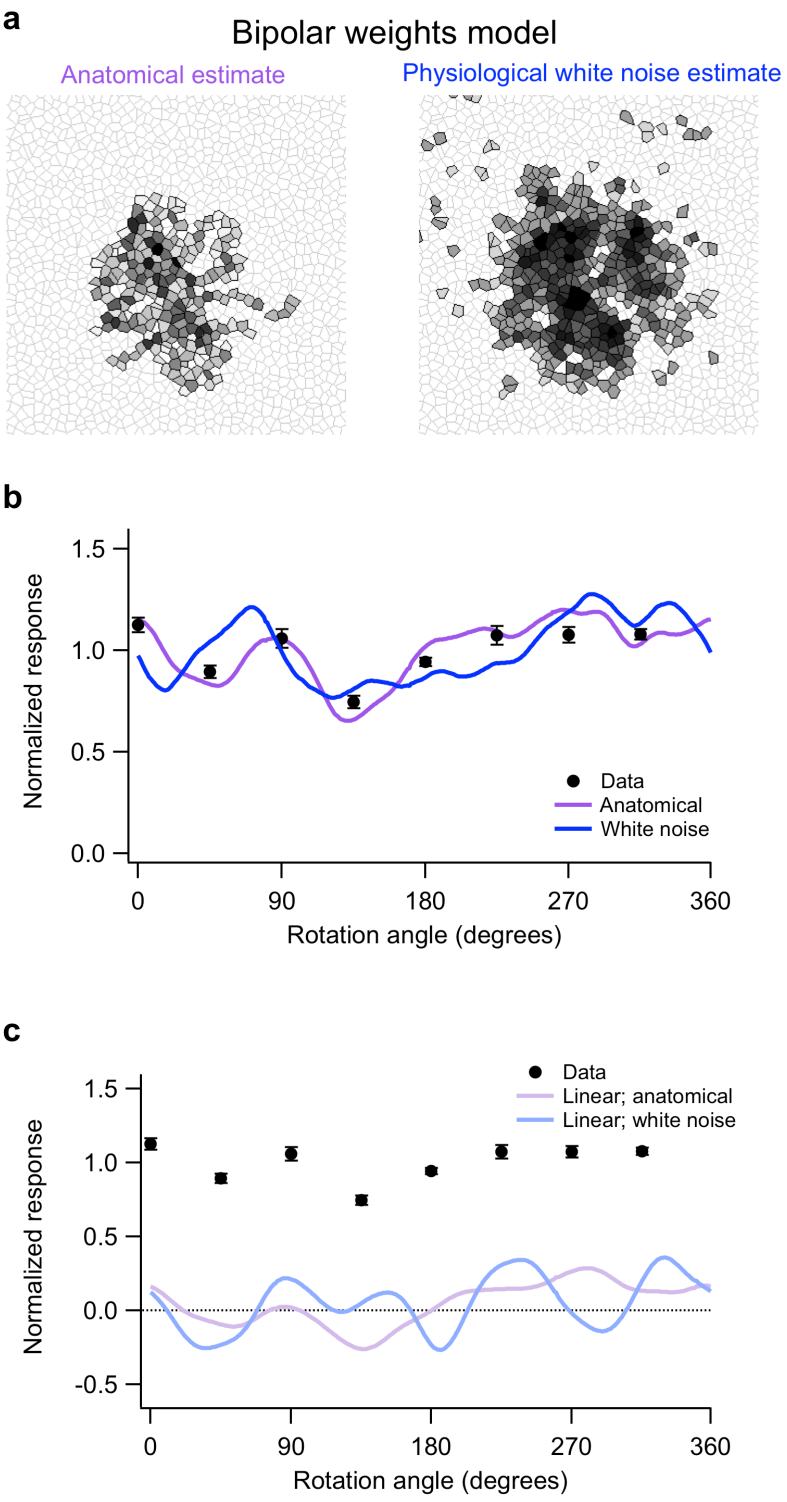

Figure S5. Anatomical verses physiological estimation of bipolar cell weights. a, Bipolar cell weight maps for the same cell as in Fig. 8 estimated using the anatomical approach or a physiological approach in which each bipolar cell is weighted by the nearest pixel in a receptive field measured from white noise stimulation with 18 µm pixels. **b**, Data (black points) and anatomical model predictions (purple curve) for rotating texture stimuli (from Fig. 8) along with the prediction from white-noise-derived bipolar cell weights (blue curve). **c**, Same as **b**, except model predictions use a linear bipolar cell output function.

Nature Neuroscience: doi:10.1038/nn.3225

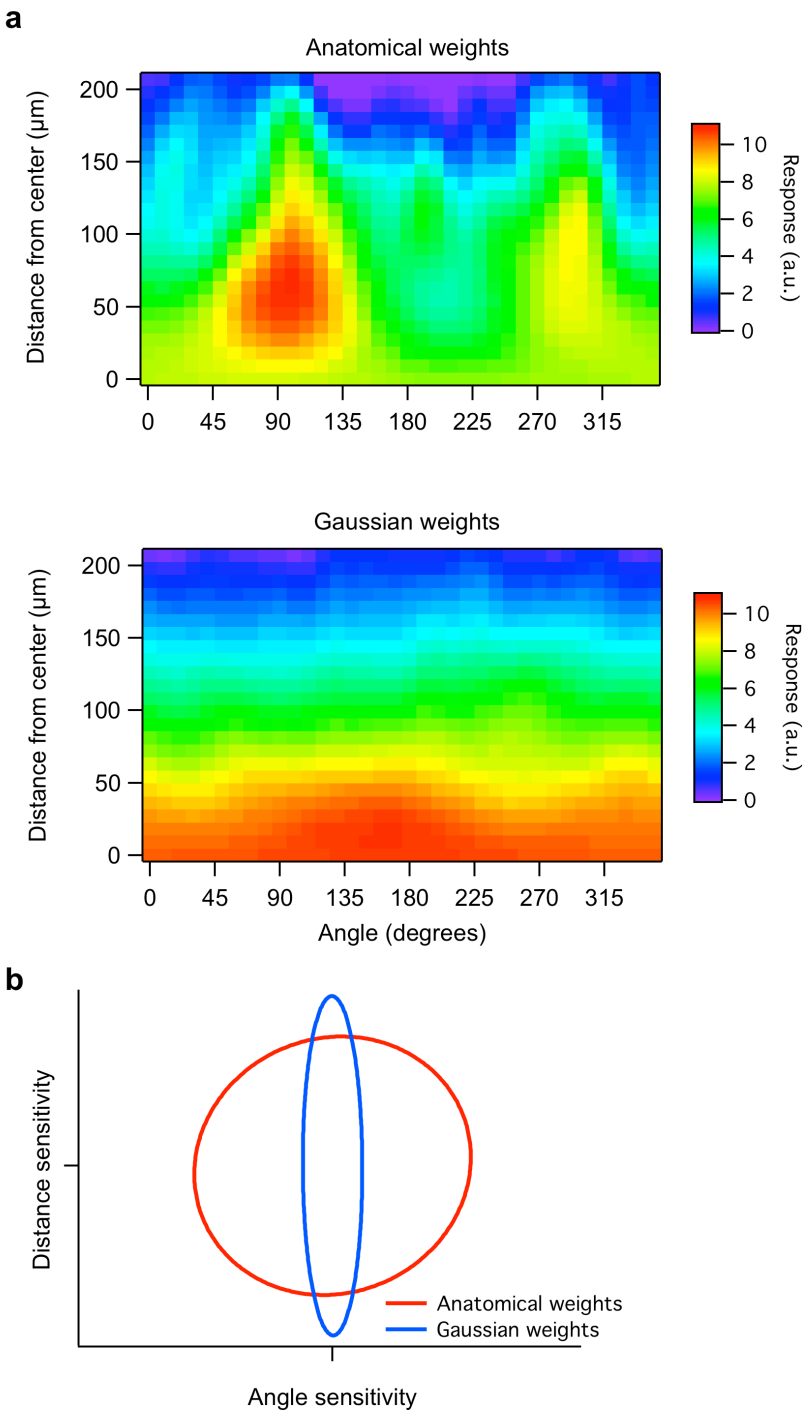

Figure S6. Information about location within the receptive field center depends on bipolar cell weight model. **a**, Model responses to 20 µm spots of light presented at various locations defined in polar coordinates as angle and distance from the center of mass of the dendritic field (see Methods). Response profiles are plotted for the anatomical-weights and for the Gaussian bipolar cell weights model in arbitrary units (a.u. with a single scale factor applied to both models). **b**, Variance ellipses representing the sensitivity of each model to the two stimulus parameters. The extent along each axis represents the stimulus dependent variance in the model. The area inside each ellipse is a measure of total stimulus dependent variance about spot location. The anatomical-weights ellipse area is larger than that of the Gaussian bipolar cell weights model by a factor of 3.51.

Nature Neuroscience: doi:10.1038/nn.3225

Cell #	Total puncta	Apposed to On bipolar	Apposed to type 6	%
1	1570	1412	967	69
2	984	831	598	72
3	1214	1111	762	69

Table S1. Statistics for type 6 bipolar cells apposed to PSD-95 puncta in On alpha-like RGCs.

Cell #	Total puncta	In type 7 territory	Apposed to type 7	%
1	1713	1471	58	3.9
2	1294	1089	16	1.5
3	1532	1231	16	1.2

Table S2. Statistics for type 7 bipolar cells apposed to PSD-95 puncta in On alpha-like RGCs.

Property	Gaussian weights model	Anatomical weights model
Bipolar output	Linear or nonlinear	Linear or nonlinear
Weights of individual synapses	Constant	Constant
Bipolar weights	Proportional to number of synapses within area of bipolar axon terminal	Proportional to number of synapses within area of bipolar axon terminal
Estimate of number of synapses	Decline smoothly with distance from soma to approximate decline in dendritic density	Determined for each model bipolar by overlap of its synaptic terminal with the RGC dendrites
Total bipolar weight (number of synapses total)	Constant	Constant
Number of bipolar cells inside dendritic field with nonzero weight	0	> 0

Table S3. Comparison of Gaussian bipolar cell weights model and anatomical bipolar cell weights model.

Captions for Supplemental Movies

Movie M1. Identifying appositions of PSD95 puncta with type 6 bipolar axon terminals. The dendritic segment shown in figure 4c-e is zoomed in and rotated in 3-D to demonstrate the identification of appositions with type 6 bipolar axon terminals. PSD95-CFP puncta, tdTomato filled alpha-like ON RGC dendrites, ON-bipolar axons labeled by YFP and Syt2 immunoreactivity are shown in green, blue, red and white, respectively. The first set of flashing white dots represent all the identified PSD95 puncta and the second set show those apposed to ON-bipolar axon terminals. The red flashing dots represent PSD95 puncta classified as apposed to type 6 bipolar cells.

Movie M2. Identifying appositions of PSD95 puncta with type 7 bipolar axon terminals. The identification of the apposition of PSD95 puncta with type 7 bipolar cells is demonstrated in 3-D in the same way as movie S1 using the dendritic segment enlarged in figure 4i-j. PSD95-CFP puncta, tdTomato filled alpha-like ON RGC dendrites, type 7 bipolar axons labeled by GFP are shown in green, blue and red, respectively. The first set of flashing white dots represents all the identified PSD95 puncta and the second set represents those apposed to type 7 bipolar cells.

Supplemental Discussion

Additional tests of model parameters

In addition to the manipulations described in the test, we tested an optimized Gaussian model that included a free parameter to shift the stimulus relative to the Gaussian profile. Such a shift improved the fit of the Gaussian model, but the predictions remained substantially worse than those from the anatomical-weights model (likelihood ratio = 10^{38}). As is evident in the example in Fig. 8b (dashed red line), the optimized Gaussian fit retains a shape that varies slowly with stimulus rotation angle and hence fails to account for large changes in response with small changes in angle. Further, the shift parameter in the optimized Gaussian is likely to over-fit the data, while we verified that the shift parameter for the anatomical-weights model was not over-fitting (Supplemental Fig. S1). Evidence for over-fitting of the optimized Gaussian model comes from the large and variable stimulus shifts required to fit the data (58 ± 60 μm); these shifts sometimes fell outside the range likely to be caused by shear in the flat-mounted retina (<40 μm as estimated from the angle of labeled bipolar cell axons as in Fig. 5b). In contrast, the stimulus shifts for the anatomical-weights model were smaller and less variable (29 ± 12 μm). Because of the likely over-fitting, the reduction in the likelihood ratio for the optimized Gaussian fit relative to the non-optimized fit is difficult to interpret. Nonetheless, for all conditions tested the anatomical-weights model fit the data more accurately than a Gaussian model.

The above considerations show that deriving bipolar cell weights from the imaged dendrites effectively imposes spatial structure on the model that is critical in predicting the RGC response. Because the axon terminal areas of type 6 bipolar cells are small in comparison to both the bipolar cell receptive field (Fig. 7b) and the heterogeneities in coverage by the RGC dendrites (see Fig. 6e), neither the precise size of the bipolar cell terminals nor their precise location in space was important to the spatial structure of the model (see shaded region in Fig. 7d).